

# Determination of Inlet Transmission and Conversion Efficiencies for in Situ Measurements of the Nocturnal Nitrogen Oxides, NO<sub>3</sub>, N<sub>2</sub>O<sub>5</sub> and NO<sub>2</sub>, via Pulsed Cavity Ring-Down Spectroscopy

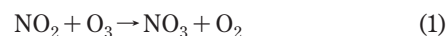
Hendrik Fuchs,<sup>†,‡</sup> William P. Dubé,<sup>†,‡</sup> Steven J. Ciciora,<sup>†</sup> and Steven S. Brown<sup>\*,†</sup>

Earth System Research Laboratory, NOAA, Boulder, Colorado 80305, and Cooperative Institute for Research in the Environmental Sciences, University of Colorado, Boulder, Colorado 80309

Pulsed cavity ring-down spectroscopy is a highly sensitive method for direct absorption spectroscopy that has been applied to in situ detection of NO<sub>3</sub>, N<sub>2</sub>O<sub>5</sub> and NO<sub>2</sub> in the atmosphere from a variety of platforms, including ships, aircraft, and towers. In this paper, we report the development of schemes to significantly improve the accuracy of these measurements. This includes the following: (1) an overall improvement in the inlet transmission efficiencies (92 ± 2% for NO<sub>3</sub> and 97 ± 1% for N<sub>2</sub>O<sub>5</sub>) achieved primarily through a reduction in the inlet residence time; and (2) the development of a calibration procedure that allows regular determination of these efficiencies in the field by addition of NO<sub>3</sub> or N<sub>2</sub>O<sub>5</sub> to the inlet from a portable source followed by conversion of NO<sub>3</sub> to NO<sub>2</sub>. In addition, the dependence of the instrument's sensitivity and accuracy to a variety of conditions encountered in the field, including variations in relative humidity, aerosol loading, and VOC levels, was systematically investigated. The rate of degradation of N<sub>2</sub>O<sub>5</sub> transmission efficiency on the inlet and filter system due to the accumulation of inorganic aerosol was determined, such that the frequency of filter changes required for accurate measurements could be defined. In the absence of aerosol, the presence of varying levels of relative humidity and reactive VOC were found to be unimportant factors in the instrument's performance. The 1  $\sigma$  accuracy of the NO<sub>3</sub>, N<sub>2</sub>O<sub>5</sub>, and NO<sub>2</sub> measured with this instrument are −9/+12, −8/+11, ± 6%, respectively, where the  $\mp$  signs indicate that the actual value is low/high relative to the measurement. The largest contribution to the overall uncertainty is now due to the NO<sub>3</sub> absorption cross section rather than the inlet transmission efficiency.

The nitrate radical (NO<sub>3</sub>) and dinitrogen pentoxide (N<sub>2</sub>O<sub>5</sub>) are key nocturnal forms of nitrogen oxides. NO<sub>3</sub> participates in the oxidation of pollutants during the night in the troposphere, <sup>1,12,24</sup> particularly of unsaturated hydrocarbons and sulfur compounds.<sup>2</sup>

Hydrolysis of N<sub>2</sub>O<sub>5</sub> on aerosol is one of the most important reactions in the conversion of nitrogen oxides to soluble nitrate (NO<sub>3</sub><sup>−</sup>) in the troposphere.<sup>10</sup> NO<sub>3</sub> is formed in the reaction of nitrogen dioxide (NO<sub>2</sub>) and ozone (O<sub>3</sub>). Since it is easily photolyzed by visible light,<sup>25</sup> appreciable levels of NO<sub>3</sub> can only accumulate in the dark. NO<sub>3</sub> is in a thermal equilibrium with N<sub>2</sub>O<sub>5</sub>, which is formed in the reaction of NO<sub>2</sub> and NO<sub>3</sub>:



Early measurements of NO<sub>3</sub> were mostly performed by long-path differential optical absorption spectroscopy (DOAS).<sup>15,19–21</sup> Since the past decade, cavity ring-down spectroscopy (CaRDS) has been developed as a highly sensitive, in situ method to detect NO<sub>3</sub><sup>13</sup> and also the sum of NO<sub>3</sub> and N<sub>2</sub>O<sub>5</sub> after the thermal decomposition of N<sub>2</sub>O<sub>5</sub> to NO<sub>3</sub> in a heated inlet.<sup>4,11,23</sup> Detection limits of in the range of a few tenths of a pptv for NO<sub>3</sub> (pptv, parts per trillion per volume) at a high temporal resolution (in the range

- (3) (a) Atkinson, R.; et al. IUPAC Subcommittee on Gas Kinetic Data Evaluation for Atmospheric Chemistry. 2003. (b) Brown, S. S. *Chem. Rev.* **2003**, *103*, 5219–5238.
- (4) Brown, S. S.; et al. *Geophys. Res. Lett.* **2001**, *28*, 3227–3230.
- (5) Brown, S. S.; et al. *Rev. Sci. Instrum.* **2002**, *73* (9), 3291–3301.
- (6) Brown, S. S.; et al. *Science* **2006**, *311*, 67–70.
- (7) Brown, S. S.; et al. *J. Geophys. Res.* **2007**, *112*.
- (8) Brown, S. S.; et al. *Atmos. Chem. Phys.* **2007**, *7*, 139–149.
- (9) Burkholder, J. B.; Talukdar, R. K. *Geophys. Res. Lett.* **1994**, *21* (7), 581–584.
- (10) Dentener, F. J.; Crutzen, P. J. *J. Geophys. Res.* **1993**, *98* (D4), 7149–7163.
- (11) Dubé, W. P.; et al. *Rev. Sci. Instrum.* **2006**, *77*, 034–101.
- (12) Geyer, A.; et al. *J. Geophys. Res.* **2001**, *106* (D8), 8013–8025.
- (13) King, M. D.; Dick, E. M.; Simpson, W. R. *Atmos. Environ.* **2000**, *35* (685–688), 4370–4375.
- (14) Liu, B. Y. H.; Lee, K. W. *Am. Ind. Hyg. Assoc. J.* **1975**, *26*, 861.
- (15) Noxon, J. F.; Norton, R. B.; Marovich, E. *Geophys. Res. Lett.* **1980**, *7*, 125–128.
- (16) Orphalv, J.; Fellows, C. E.; Flaud, P. J. *Geophys. Res.* **2003**, *108* (D3), 4077.
- (17) Osthoff, H.; et al. *J. Geophys. Res.* **2006**, *111* (24).
- (18) Osthoff, H.; et al. *Phys. Chem. Chem. Phys.* **2007**, *9*, 5785–5793.
- (19) Plane, J. M. C.; Nien, C. *Rev. Sci. Instrum.* **1992**, *63*, 1867–1876.
- (20) Platt, U.; Heintz, F. *Israel J. of Chem.* **1994**, *34*, 289–300.
- (21) Platt, U.; et al. *Geophys. Res. Lett.* **1980**, *7*, 89–92.
- (22) Sander, S. P.; et al. *NASA JPL Publ.* **2006**, 06–2.
- (23) Simpson, R. J. *Rev. Sci. Instrum.* **2003**, *74* (7), 3442–3452.
- (24) Warneke, C. et al. *J. Geophys. Res.* **2004**, *109*, 309.
- (25) Wayne, R. P.; et al. *Atmos. Environ.* **1991**, *25* (1), 1–203.

\* To whom correspondence should be addressed. E-mail: steven.s.brown@noaa.gov. Fax: (303) 497 5126.

<sup>†</sup> NOAA.

<sup>‡</sup> University of Colorado.

(1) Aldener, M.; et al. *J. Mol. Spectrosc.* **2007**, *232*, 223–230.

(2) Atkinson, R. J. *Phys. Chem. Ref. Data* **1991**, *20*, 459.

of seconds) can be reached for CaRDS. In contrast to the DOAS technique, CaRDS instruments sample air into a closed cavity, so that measured concentrations have to be corrected for losses of NO<sub>3</sub> on surfaces. This places a limitation on the accuracy of the measurement.

The NOAA CaRDS instruments for detection of NO<sub>2</sub>, NO<sub>3</sub>, and N<sub>2</sub>O<sub>5</sub><sup>11,17</sup> have been successfully deployed in several aircraft and ship missions<sup>6,7</sup> as well as at ground sites and at a tall tower.<sup>8</sup> This article reports the further developments of these instruments that have led to a significant improvement in their accuracy. The improvements include the following: changes in the instrument's NO<sub>2</sub> detection scheme to allow not only for monitoring of ambient NO<sub>2</sub> but also for periodic determination of the transmission efficiencies for NO<sub>3</sub> and N<sub>2</sub>O<sub>5</sub> via their conversion to NO<sub>2</sub>; changes to the inlet system to reduce the total residence time; and quantification of inlet transmission efficiencies through a series of laboratory tests. The latter involved a systematic investigation of the possible changes of the instrument's sensitivity and accuracy under a variety of conditions representative of those encountered in the field.

## INSTRUMENT OVERVIEW

A description of the detection principle and operating characteristics of these instruments have been given elsewhere;<sup>5,11,17</sup> they are briefly summarized in the beginning of this section for completeness.

CaRDS has become an established direct absorption technique to measure atmospheric trace gas concentrations.<sup>3</sup> In our case, a nanosecond scale laser pulse is coupled into a high-finesse cavity and the intensity of the light transmitted through the end mirror of the cavity is observed. The intensity ( $I(t)$ ) decays as a single exponential with a time constant ( $\tau$ ). The detector's background signal is measured prior to the laser pulse and subtracted so that  $\tau$  can be derived from a standard linear fit of the logarithmic signal:

$$I(t) = I_0 \exp(-t/\tau) \quad (3)$$

The measurement of a trace gas concentration ( $[A]$ ) is accomplished by comparing the fitted ring-down time constants in the presence ( $\tau$ ) and absence of the absorber ( $\tau_0$ ) using the absorption cross section ( $\sigma_A$ ) at the probing wavelength:

$$[A] = \frac{R_L}{c\sigma_A} \left( \frac{1}{\tau} - \frac{1}{\tau_0} \right) \quad (4)$$

Here,  $c$  is the speed of the light and  $R_L$  is the ratio of the total cavity length to the length over which the absorber is present in the cavity. The background time constant ( $\tau_0$ ) is limited by mirror reflectivity, Rayleigh and Mie scattering of the gas and aerosol present in the cavity, and absorption due to trace gases other than the target absorber.

Figure 1 shows the layout of the NOAA aircraft CaRDS instrument, which is capable of measuring NO<sub>3</sub>, N<sub>2</sub>O<sub>5</sub> and NO<sub>2</sub> concentrations simultaneously. The extinction of the sampled air at 662 nm is measured in two separate cavities. A 6-ns laser pulse (0.5-mJ pulse energy, 50-Hz repetition rate) at 662 nm is generated by a ND:YAG (Big Sky Laser, ultra CFR) pumped dye laser (Dakota Technology, Northern Lights). The dye laser wavelength

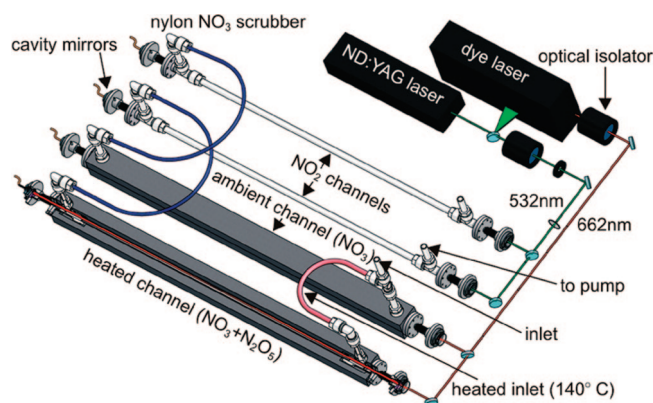


**Figure 1.** Schematic of the four-channel cavity ring-down instrument for measurements of ambient NO<sub>3</sub>, N<sub>2</sub>O<sub>5</sub>, and NO<sub>2</sub> concentrations.

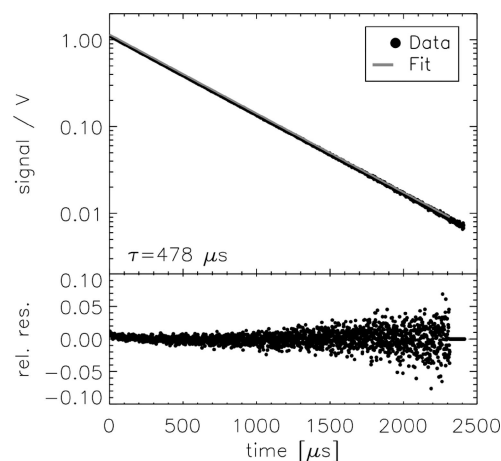


**Figure 2.** Example ring-down trace at 662 nm for 1-s integration time. The lower panel shows the relative residual to the fitted single-exponential decay with a ring-down time constant of 478  $\mu$ s.

(line width 0.5 cm<sup>-1</sup>) is tuned out of resonance with any of the weak water vapor absorption lines (line width  $\sim$ 0.3 cm<sup>-1</sup> at atmospheric pressure,<sup>1</sup>) that lie underneath the peak of the 80-cm<sup>-1</sup>-wide NO<sub>3</sub> band centered near 662 nm. The laser light is coupled into the cavity (mirror reflectivity, 99.9995%; transmission,  $\leq$ 5 ppmv; curvature, 1 m; distance, 93 cm) after propagating through an optical isolator and a series of irises and lenses to minimize the spot size at the far end of the cavity. Light transmitted through the rear mirror is collected using an optical fiber and is imaged on to a small photomultiplier tube through a band-pass filter. Figure 2 shows an example ring-down trace recorded on a digital oscilloscope card at 16-bit resolution. The precision of the ring-down time constants gives the limit of detection ( $2\sigma$ ) of the instrument in terms of extinction coefficient to  $1 \times 10^{-10}$  cm<sup>-1</sup>, similar to what has been reported previously.<sup>11</sup>

The measurement of the ring-down time constant without the absorber, which must be known to derive trace gas concentrations (eq 3), is accomplished by periodic addition of excess NO to the inlet to chemically destroy NO<sub>3</sub> via the reaction NO<sub>3</sub> + NO  $\rightarrow$  2NO<sub>2</sub>. This zeroing method is highly specific to determine the extinction at 662 nm from all contributions other than NO<sub>3</sub> absorption. A 40 sccm flow of a mixture of 100 ppmv NO in nitrogen is added for 5 s every 3–5 min. This yields an NO mixing ratio of 0.5 ppmv in the sampled air, which is sufficient to

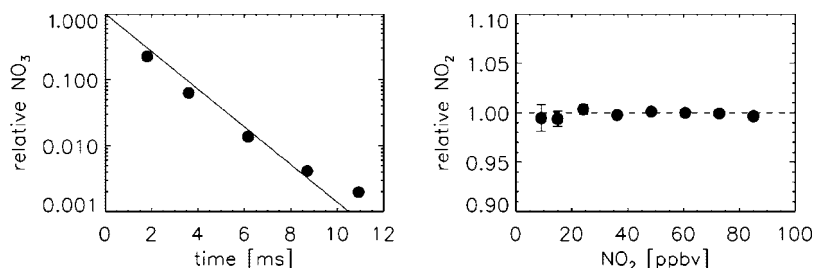


**Figure 3.** Left panel: relative NO<sub>3</sub> concentration vs residence time in  $1/4$ -in. Nylon 11 tubing showing that this material is an effective scrubber for NO<sub>3</sub>. Right panel: transmission of NO<sub>2</sub> through a 95-cm length of Nylon 11 tubing as a function of NO<sub>2</sub> mixing ratio. The average transmission is  $99.8 \pm 0.3\%$ , amounting to a negligible loss for NO<sub>2</sub>.

completely titrate NO<sub>3</sub> in the system before it enters the cavities (NO<sub>3</sub> first-order loss rate coefficient  $110 \text{ s}^{-1}$ ).

A key difference in the current instrument is a decreased residence time due largely to sampling at reduced pressure and due to using smaller diameter cavities and tubing (reduced from  $3/8$ -in. (9.5 mm) to  $1/4$ -in. (6.4 mm) i.d.). The total flow through the instrument is 8 slm (slm, liter per minute at standard pressure and temperature) of ambient air, which is sampled through 0.3–0.4-m length of  $1/8$ -in.-o.d. Teflon tubing that serves as restriction leading to a reduced pressure of  $\sim 350$  hPa inside the instrument. The instrument can be operated under active pressure control (MKS type 640), in which a small fraction of the total flow is diverted directly to the pump downstream of the pressure restriction.

There are several advantages to operation at reduced pressure. First, the residence time through the inlet and optical cavities is shorter, minimizing the wall loss of NO<sub>3</sub> and N<sub>2</sub>O<sub>5</sub>. Second, the number density of other reactive trace gases and water vapor is reduced such that they are less likely to either react with NO<sub>3</sub> or adsorb to the walls of the inlet. Third, liquid water may evaporate at lower pressure and is less likely condensed on wall surfaces and aerosol where it could enhance wall and filter loss of NO<sub>3</sub> and N<sub>2</sub>O<sub>5</sub>. Fourth, Rayleigh scattering becomes smaller so that the ring-down time constant and therefore the effective optical path length is increased. This advantage is only important if the contribution of Rayleigh scatter to the overall light loss in the cavity is significant compared to the other losses such as the mirror transmission (e.g., for the instrument described here, losses due to both mirror reflectivity and Rayleigh scattering at 1 atm are both  $\sim 5$  ppm per pass). The reduced pressure does not change the Reynolds number for given mass flow rate and therefore does not introduce additional turbulence, which can lead to optical noise in the measurement. However, the reduced pressure has the disadvantage of reduced number density of the target absorber so that  $2\sigma$  limits of detection are slightly increased (NO<sub>3</sub>, 0.6 pptv; N<sub>2</sub>O<sub>5</sub>, 2 pptv; NO<sub>2</sub>, 200 pptv) compared to previously reported values.<sup>11,17</sup>

The sampled air passes through a Teflon filter (PTFE,  $2\text{-}\mu\text{m}$  pore size,  $25\text{-}\mu\text{m}$  thick) to remove particles that can significantly contribute to the extinction measured in the cavity. The filter is exchanged regularly (every 0.5–3 h) by a fully automated filter changer.<sup>11</sup> The sampled air is divided into two 4 slm flows downstream of the filter. One flow passes through a two-stage heater to thermally convert N<sub>2</sub>O<sub>5</sub> to NO<sub>3</sub> (see below for details) and into a cavity maintained at  $75^\circ\text{C}$ . The other part of the

sampled air enters the second cavity, which is maintained at ambient temperature using an actively cooled, aluminum manifold that surrounds the Teflon tubing.

Turbulators (additional flow restrictions consisting of a short length of twisted,  $1/4$ -in.-o.d. Teflon tubing inserted into the  $3/8$ -in. tubing) are present in the tubing upstream of the cavities to ensure that the air is well mixed.

A second important difference from the previous versions of this instrument is the presence of two additional cavities downstream of each of the 662-nm cavities in which the extinction of the sampled air at 532 nm is measured, according to the method described by ref 17. A small part (5%) of the ND:YAG laser output is split from the beam that pumps the dye laser and is coupled into these cavities (mirror reflectivity, 99.999%). The geometrical design of the 532-nm cavities and the data acquisition are similar to that of the 662-nm cavities. These additional channels are used to measure atmospheric NO<sub>2</sub> concentrations and also to determine the NO<sub>3</sub> losses in the system as described in more detail below.

A 95-cm length of Nylon 11 tubing, which serves as a scrubber for NO<sub>3</sub>, is placed between each 662- and 532-nm cavity. It is necessary to destroy the NO<sub>3</sub> between the cavities because its absorption cross section at 532 nm is more than 1 order of magnitude larger than that of NO<sub>2</sub>.<sup>26</sup> Figure 3 (left panel) shows the loss of NO<sub>3</sub> on the Nylon tubing measured by observing the NO<sub>3</sub> extinction at 662 nm transmitted through various lengths of the Nylon tubing (first order loss rate,  $90 \pm 10 \text{ s}^{-1}$ ). Thus, a 95-cm length of Nylon tubing was found to remove NO<sub>3</sub> below the level where its optical extinction was detectable at 532 nm. The reaction of NO<sub>3</sub> with the Nylon surfaces does not lead to NO<sub>2</sub> production. This was checked by comparing the NO<sub>2</sub> measured in the two 532-nm cavities when NO<sub>3</sub> was scrubbed by Nylon upstream of one of the cavities and titrated via NO upstream of the other cavity. The difference between both NO<sub>2</sub> measurements were consistent with the increase of NO<sub>2</sub> from the titration of NO<sub>3</sub>, whose concentration was measured in the 662-nm cavities. Loss of NO<sub>2</sub> on the NO<sub>3</sub> scrubber was checked by connecting the two NO<sub>2</sub> channels with a 95-cm length of Nylon tubing and comparing the measurements of NO<sub>2</sub> in dry zero air. Although this measurement was carried out in dry zero air, and so potentially neglects effects such as conversion of NO<sub>2</sub> to HONO on surfaces, recent field comparisons of this instrument to other NO<sub>2</sub> measurements under conditions of varying relative humidity have not revealed any humidity-dependent artifacts (Fuchs, H., manuscript in

(26) Yokelson, R. J.; et al. *J. Phys. Chem.* **1994**, *98*, 13, 144–150.



preparation). Figure 3 (right panel) shows that loss of NO<sub>2</sub> is less than 0.3% through the scrubber. Transmission of ozone (not shown here) was also quantitative to within 1%.

As described previously,<sup>17</sup> the determination of the  $\tau_0$  at 532 nm is accomplished by overflowing the inlet with zero air. Although this zero method for NO<sub>2</sub> is not as specific as the NO titration for NO<sub>3</sub>, the only interference that we are aware of is optical extinction due to ozone (the ozone absorption cross section is ~50 times smaller than that of NO<sub>2</sub> at 532 nm<sup>9</sup>). Therefore, 532-nm extinction due to ozone absorption must be calculated from a separate ozone measurement and subtracted from the total extinction in order to determine the NO<sub>2</sub> concentration.

## INSTRUMENT CHARACTERIZATION

**Effective Path Length  $R_L$ .** The calculation of the absorber's concentration (eq 3) requires the knowledge of the ratio between the absorption path length and the distance between the mirrors,  $R_L$ . This ratio is reduced compared to the distance of the mirrors because the volumes adjacent to the mirrors are purged with a small flow of dry synthetic air (zero air) to keep them clean. An overall flow of 200 sccm of zero air is divided into nearly equal parts for each of the eight cavity mirrors using a single-flow controller and eight critical orifices.

The ratio of the absorption path length and the mirror distance cannot be derived simply from the distance between the inlet and outlet of the sampled gas and the distance between the mirrors (ratio 1.24), because part of the sampled gas penetrates the purge volumes. Therefore,  $R_L$  was determined by the measurement of a known concentration of ozone, which was produced and measured (mixing ratio, 10–500 ppbv) by a standard ozone monitor. This was compared to the ozone absorption measured in each cavity by its visible optical absorption in the Chappius bands. The fitted slopes (1.14) were similar for all channels with an uncertainty of 3% due to the ozone monitor (2%) and the absorption cross section (1%).

**Conversion of N<sub>2</sub>O<sub>5</sub> to NO<sub>3</sub>.** The instrument has two channels in which the extinction of the sampled air at 662 nm is measured, one of which is heated to induce thermal decomposition of N<sub>2</sub>O<sub>5</sub> to NO<sub>3</sub> in order to determine the sum of both trace gas concentrations. The conversion is achieved upstream of the cavity in a two-stage heater system consisting of heated 3/8-in. o.d. (1/4-in. i.d.) Teflon tubing. The first zone (length 31 cm) is kept at a temperature of 140 °C (outside wall temperature) to heat the gas rapidly to temperatures that ensures that the equilibrium is shifted toward NO<sub>3</sub>. The second zone (80 °C, length 16 cm) serves as a relaxation zone to bring the gas temperature close to that inside the cavity in order to avoid temperature gradients and thereby reduce turbulent flow noise.

The sample volume inside the cavity of this channel is heated to a constant temperature of 75 °C, which is sufficient to maintain the equilibrium between the two species on the side of NO<sub>3</sub> for typical atmospheric concentrations of NO<sub>2</sub>. The ratio of NO<sub>3</sub> to N<sub>2</sub>O<sub>5</sub> at this temperature depends linearly on the NO<sub>2</sub> mixing ratio in the sampled air. Measurements are corrected for this small equilibrium effect by calculating the fraction of N<sub>2</sub>O<sub>5</sub> + NO<sub>3</sub> remaining as N<sub>2</sub>O<sub>5</sub> (1% per 10 ppbv NO<sub>2</sub> calculated from the equilibrium constant<sup>3,22</sup>).

The temperature of the heating zone 1 was optimized in laboratory experiments sampling air containing N<sub>2</sub>O<sub>5</sub> from a

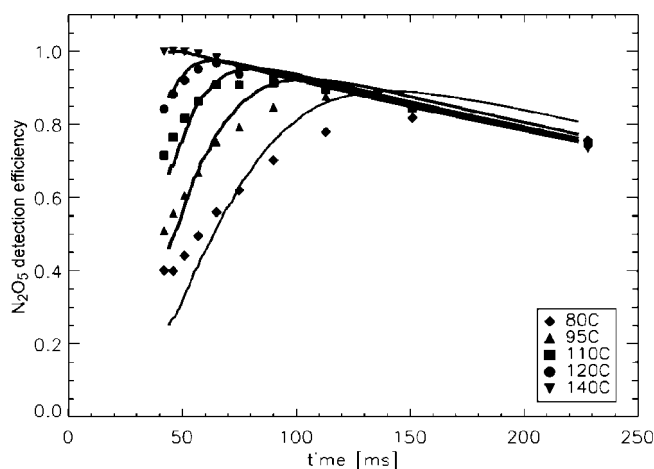


**Figure 4.** Measured dependence of N<sub>2</sub>O<sub>5</sub> detection efficiency (i.e., the product of the conversion efficiency of N<sub>2</sub>O<sub>5</sub> to NO<sub>3</sub> and the transmission efficiency of NO<sub>3</sub> through the inlet downstream of the N<sub>2</sub>O<sub>5</sub> conversion) on the heater temperature and residence time (symbols). The residence time was varied by changing the flow rate. Measurements are compared with results of simple model calculations (solid lines, see text).

calibration source (see below). The residence time of the sampled air in the heater and the heater temperature were systematically varied. The first was achieved by manipulating the flow rates in both channels simultaneously so that only the residence time in the heater and cavity was changed but not the overall flow conditions in the inlet and filter system upstream of the cavities. The residence time was calculated from the flow rate by assuming plug flow conditions.

The relative NO<sub>3</sub> absorption signal in the heated 662-nm channel as a function of residence time for different heater temperatures gives a measurement of the relative conversion efficiency of N<sub>2</sub>O<sub>5</sub> in the system (Figure 4). It shows a distinct maximum as a function of residence time in the heater at a fixed heater temperature. In addition, this maximum increases and is shifted toward shorter residence times with higher heater temperature. This can be understood as a competition between thermal decomposition of N<sub>2</sub>O<sub>5</sub>, limited primarily by heat transfer rather than the unimolecular decomposition rate coefficient of N<sub>2</sub>O<sub>5</sub>, and NO<sub>3</sub> loss on Teflon surfaces at longer residence times.

These results were confirmed qualitatively by model calculations (solid lines in Figure 4) that were constrained by an inlet temperature profile and included a first-order NO<sub>3</sub> wall loss ( $k = 0.3 \pm 0.1 \text{ s}^{-1}$ ; see below). Results are independent of the initial N<sub>2</sub>O<sub>5</sub> mixing ratio at the tip of the inlet.

A temperature of 140 °C of the converter and a flow rate of 4 slm lead to a maximum conversion efficiency. Together with the results of the absolute transmission efficiencies measurements for N<sub>2</sub>O<sub>5</sub> of 98% (see below), this configuration allows for optimum conversion of N<sub>2</sub>O<sub>5</sub> to NO<sub>3</sub>.

In contrast to the heated channel, the ambient channel used for the measurement of NO<sub>3</sub> is actively cooled to keep the gas temperature similar to ambient temperature. This suppresses unwanted thermal decomposition of N<sub>2</sub>O<sub>5</sub> to NO<sub>3</sub> and prevents optical noise arising from thermal gradients within the ambient channel. However, under conditions of excessive heat load (e.g., aircraft sampling, in which the fuselage temperature may be higher than the ambient temperature outside the aircraft), the

temperature of the  $\text{NO}_3$  measurement channel may deviate from ambient. In this case, a factor is applied for the  $\text{N}_2\text{O}_5$  thermal decomposition within the inlet. For aircraft measurements, in which the temperature gradients are most severe, the average value of this correction factor is 2% but can be larger (e.g., 20%) for large  $\text{NO}_x$  plumes ( $>25$  ppbv).

**Determination of Inlet Transmission Efficiencies.**  $\text{NO}_3$  and  $\text{N}_2\text{O}_5$  are reactive species. Therefore, losses in the inlet system and inside the cavity have to be quantified in order to correct concentrations measured inside the cavity to actual, ambient concentrations. The correction for  $\text{NO}_3$  is straightforward because the  $\text{NO}_3$  concentration is directly measured by its extinction at 662 nm:

$$[\text{NO}_3]_{\text{amb}} = \frac{[\text{NO}_3]_{\text{meas}}}{T_E(\text{NO}_3)} \quad (5)$$

$T_E(\text{NO}_3)$  is the transmission efficiency for  $\text{NO}_3$  in the ambient channel.

In contrast, the heated channel measures the sum of  $\text{N}_2\text{O}_5$  and  $\text{NO}_3$ . Only that part of the sum signal that refers to  $\text{N}_2\text{O}_5$  must be corrected for the  $\text{N}_2\text{O}_5$  losses by the  $\text{N}_2\text{O}_5$  transmission efficiency  $T_E(\text{N}_2\text{O}_5)$ . It is therefore necessary to subtract the ambient  $\text{NO}_3$  concentration prior to the  $\text{N}_2\text{O}_5$  correction. However, the  $\text{NO}_3$  transmission efficiency in the sum channel ( $T_E'(\text{NO}_3)$ ) may differ from that of the ambient  $\text{NO}_3$  channel ( $T_E(\text{NO}_3)$ ):

$$[\text{N}_2\text{O}_5]_{\text{amb}} = \frac{1}{T_E(\text{N}_2\text{O}_5)} \left( ([\text{NO}_3] + [\text{N}_2\text{O}_5])_{\text{meas}} - T_E'(\text{NO}_3) [\text{NO}_3]_{\text{amb}} \right) \quad (6)$$

Thus, three different inlet transmission efficiencies (eqs 5 and 6) have to be known to calculate the ambient  $\text{N}_2\text{O}_5$  concentration from the two measured extinctions. These were determined via two different methods.

The first method was direct measurement of  $\text{NO}_3$  and  $\text{N}_2\text{O}_5$  losses on various components of the inlet system. First, reactive species are lost on the surface of the Teflon tubing. This can be described as a first-order loss process, since previous work has shown that the  $\text{NO}_3$  loss scales with inlet residence time.<sup>5,11</sup> Second,  $\text{NO}_3$  and  $\text{N}_2\text{O}_5$  are also lost on the filter, which acts as a fixed, point loss in the system. The loss in the latter was measured by comparing the  $\text{NO}_3$  absorption from the  $\text{NO}_3$  or  $\text{N}_2\text{O}_5$  source sampled through the entire inlet including the filter system to that obtained by bypassing the filter system with a short piece of Teflon tubing. This yielded in a loss of  $\text{NO}_3$  in the filter system of  $5 \pm 2\%$  and no significant loss of  $\text{N}_2\text{O}_5$ . Total loss on the filter and its housing are now considerably smaller than previously reported ( $10 \pm 5\%$ ,<sup>11</sup>), due largely to improvements in the machining process of the filter housing and reductions in the residence time.

The first-order loss rate of  $\text{NO}_3$  on  $3/8$ -in.o.d. Teflon tubing was determined by measuring the  $\text{NO}_3$  concentrations as a function of tubing length. A linear fit of the logarithmic extinction depending on the residence time in the additional tubing yielded in a loss rate of  $0.3 \pm 0.1 \text{ s}^{-1}$  consistent with previous measurements in slightly larger diameter tubing ( $1/2$ -in. o.d.,  $0.2 \pm 0.1 \text{ s}^{-1}$ ,<sup>11</sup>). This results in a wall loss of  $\text{NO}_3$  in the ambient channel of  $3 \pm 1\%$  at a residence time of 100 ms between the filter

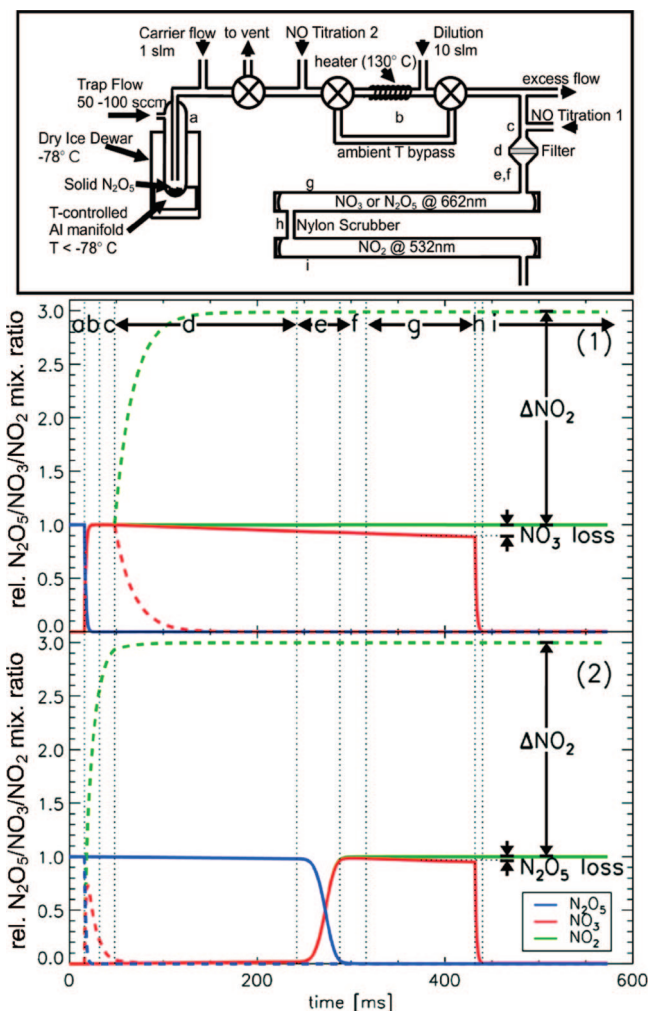


**Figure 5.** Schematic of the  $\text{NO}_3$  and  $\text{N}_2\text{O}_5$  source (upper panel) used to calibrate inlet transmission efficiency for  $\text{NO}_3$  (1) and  $\text{N}_2\text{O}_5$  (2). Graphs show the predicted time dependence of  $\text{NO}_3$ ,  $\text{N}_2\text{O}_5$ , and  $\text{NO}_2$  if the instrument (d, inlet system and filter; e/f, heater zone 1/2; g,  $\text{NO}_3$  cavity; h,  $\text{NO}_3$  scrubber; i,  $\text{NO}_2$  cavity) samples from the  $\text{N}_2\text{O}_5$  calibration source (a, cold source; b, heater; c, connection to the instrument). Dashed lines refer to the zeroing mode when excess  $\text{NO}$  is added upstream of the instrument. Heater zones e, f are present only for the  $\text{N}_2\text{O}_5$  channel. The calibration heater b is bypassed for the  $\text{N}_2\text{O}_5$  calibration but used for the corresponding zeroing mode (see text for details).

and the center of the cavity. Together with the  $\text{NO}_3$  loss on the filter, the overall  $\text{NO}_3$  transmission is  $92 \pm 2\%$ . Although this measurement was made in dry, particle-free air, the experiments described below show that the number is also applicable to ambient air that contains water vapor, aerosol, and other reactive trace gases.

In the case of  $\text{N}_2\text{O}_5$ , the only significant wall loss occurs subsequent to its conversion to  $\text{NO}_3$  downstream of the heater, since  $\text{N}_2\text{O}_5$  itself is less reactive toward Teflon surfaces. Thus, the  $\text{N}_2\text{O}_5$  transmission efficiency is  $97 \pm 1\%$  at the given residence of 100 ms between the heater and the center of the cavity.

A second approach to determine inlet transmission efficiencies is via conversion of  $\text{NO}_3$  or  $\text{N}_2\text{O}_5$  to  $\text{NO}_2$ . We have used this method to develop a calibration suitable for use in both the laboratory and the field (Figure 5). The calibration system consists of a solid  $\text{N}_2\text{O}_5$  sample kept at a constant temperature below  $-78$

°C (dry ice). This is accomplished by actively cooling the glass trap containing the crystalline  $\text{N}_2\text{O}_5$  with a Peltier-cooled aluminum housing attached to a heat sink, all of which is immersed in a dry ice/2-propanol bath. A small flow of zero air ( $\sim 50$  sccm) is passed over the crystalline solid to produce a flow that is saturated with  $\text{N}_2\text{O}_5$  at its vapor pressure at the chosen temperature. This flow is maintained in order to keep the output from this source more stable and can be diverted to a vent line during periods when calibration measurements are not being performed. A carrier flow of 1 slm ensures a rapid transport from the trap to the inlet of the instrument. The  $\text{N}_2\text{O}_5$  is further diluted by  $\sim 10$  slm of zero air just prior the instrument's inlet so that typical  $\text{N}_2\text{O}_5$  mixing ratios used for the calibration measurements are  $\sim 1$  ppbv. As shown in Figure 5, the flow from the  $\text{N}_2\text{O}_5$  source can be directed through a heater at  $130^\circ\text{C}$  in order to deliver  $\text{NO}_3$  instead of  $\text{N}_2\text{O}_5$ .

The  $\text{N}_2\text{O}_5$  concentration supplied by the calibration source should be a constant determined by the vapor pressure of crystalline  $\text{N}_2\text{O}_5$  at the set temperature of the trap. However, in practice, this is true only under ideal conditions; in general, the output of the  $\text{N}_2\text{O}_5$  trap at a given temperature tends to vary somewhat with time and with the age of the sample. Therefore, rather than using the  $\text{N}_2\text{O}_5$  (or  $\text{NO}_3$ ) concentration supplied by the trap as an absolute standard for calibration purposes, the in-field calibration scheme is a comparison of two measurements, one for  $\text{NO}_3$  and one for  $\text{NO}_2$  converted from  $\text{NO}_3$  via reaction with  $\text{NO}$ .

Figure 5 shows a model calculation of relative  $\text{NO}_3$ ,  $\text{N}_2\text{O}_5$ , and  $\text{NO}_2$  concentrations as a function of time during the flow through the inlet for calibration of either  $\text{NO}_3$  or  $\text{N}_2\text{O}_5$  losses (distinguished by solid or dashed lines) including the different parts of the calibration source and the instrument (indicated by the dashed vertical lines).

The middle panel of Figure 5 describes the determination of the  $\text{NO}_3$  transmission efficiency in either the heated or the ambient channels. The  $\text{N}_2\text{O}_5$  from the source (a) is thermally decomposed to  $\text{NO}_3$  and  $\text{NO}_2$  (b) upstream of the inlet system of the instrument (c). First,  $\text{NO}_3$  and  $\text{NO}_2$  concentrations are measured in the 662-nm cavity (g) and the 532-nm cavity (i), respectively (solid lines). The concentration of  $\text{NO}_3$  is reduced by losses on the filter, the filter housing (d), the Teflon tubing upstream of the cavity (e,f), and in the cavity itself (g).  $\text{NO}_3$  is removed quantitatively on the Nylon tubing (h) between the two cavities. Second,  $\text{NO}_3$  is titrated by excess  $\text{NO}$  added upstream of the inlet (c) (dashed lines), leading to the production of two  $\text{NO}_2$  for every  $\text{NO}_3$ . The difference between the two  $\text{NO}_2$  measurements (with and without  $\text{NO}$  titration) is twice the  $\text{NO}_3$  concentration present at the tip of the inlet. The ratio between the  $\text{NO}_3$  concentration measured in the calibration mode without  $\text{NO}$  titration and half of the difference of the two measured  $\text{NO}_2$  concentrations,  $\Delta[\text{NO}_2]$ , gives the  $\text{NO}_3$  transmission efficiency  $T_E(\text{NO}_3)$ :

$$T_E(\text{NO}_3) = \frac{[\text{NO}_3]}{0.5\Delta[\text{NO}_2]} \quad (7)$$

A similar calibration scheme can be applied to determine the  $\text{N}_2\text{O}_5$  transmission and conversion efficiency (Figure 5 lower panel) using the calibration source in its  $\text{N}_2\text{O}_5$  mode. First,  $\text{N}_2\text{O}_5$  and  $\text{NO}_2$  concentrations are measured in the two cavities (g, i).

These are again compared to the  $\text{NO}_2$  concentration, if  $\text{N}_2\text{O}_5$  is converted to  $\text{NO}_2$  upstream of the inlet system. Therefore, the  $\text{N}_2\text{O}_5$  is directed through the heater within the calibration source (b), which was bypassed during the first measurement, to be converted to  $\text{NO}_3$ , which reacts with added excess  $\text{NO}$  to form  $\text{NO}_2$  in a 2:1 ratio. The ratio of the measured  $\text{N}_2\text{O}_5$  concentration and half of the difference of the two measured  $\text{NO}_2$  concentrations gives the  $\text{N}_2\text{O}_5$  transmission efficiency:

$$T_E(\text{N}_2\text{O}_5) = \frac{[\text{N}_2\text{O}_5]}{0.5\Delta[\text{NO}_2]} \quad (8)$$

The calibration resulted in a transmission efficiency of  $90 \pm 3\%$  for  $\text{NO}_3$  in both the ambient and heated channels and of  $98 \pm 3\%$  for  $\text{N}_2\text{O}_5$ . The precision of these values is given by repeated measurements in the laboratory. These determinations are in agreement with the sum of the measurements of the losses on individual components of the inlet system described above.

The calibration source has been operated successfully in the field as well as the laboratory. For example, calibrations were carried out before and after each flight during the deployment of the aircraft instrument on the NOAA *P3* during the Texas Air Quality Study in August–October 2006 in Houston, TX. Measured transmission efficiencies for  $\text{NO}_3$  were on average somewhat lower than those described here (84%), but  $\text{N}_2\text{O}_5$  conversion efficiencies were similar. The decreased  $\text{NO}_3$  transmission efficiencies were consistent with the inlet residence times, which were somewhat longer with the inlet design used in that campaign than those described in this paper.

## SENSITIVITY TO AEROSOL, VOC, AND WATER VAPOR

We investigated the sensitivity of the instrument against several possible loss processes that could result from sampling in ambient air (rather than dry, synthetic air), including water vapor, aerosols, and VOCs. All test experiment described in this section were performed by using the in-field calibration system as a source for either  $\text{NO}_3$  or  $\text{N}_2\text{O}_5$ . Different contaminants were added to the dilution flow of the calibration system, and measured extinctions with and without the contaminants were compared.

Furthermore, the sensitivity of the  $\text{N}_2\text{O}_5$  transmission efficiency to humidified air, which could introduce wall losses that are not accounted for by the investigations described in the previous section, was determined. The relative humidity of the air used for the dilution of  $\text{N}_2\text{O}_5$  sampled from the calibration source was varied by mixing a flow of air saturated with water vapor that had been bubbled through a liquid water sample with dry zero air. Relative humidity was measured by a standard capacitive hygrometer.  $\text{N}_2\text{O}_5$  concentrations at different relative humidities (up to 95% at room temperature (293 K)) were compared to the concentration in dry zero air. The concentration was invariant with relative humidity to within 0.7%. This confirms that  $\text{N}_2\text{O}_5$  hydrolysis on Teflon surfaces does not affect the  $\text{N}_2\text{O}_5$  measurement. This might be partly due to the fact that the pressure in the system is significantly reduced so that the partial pressure of water vapor inside the instrument was smaller than that in the ambient air.

Accumulation of aerosol on the inlet filter could result in variable loss of  $\text{N}_2\text{O}_5$  (or  $\text{NO}_3$ , depending on the aerosol type).



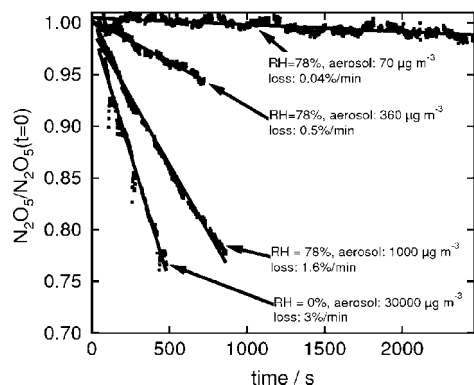


**Figure 6.** Measured  $\text{N}_2\text{O}_5$  loss for sampling of inorganic aerosol  $(\text{NH}_4)_2\text{SO}_4$  in humidified zero air ( $\text{RH} = 78\%$ ) and dry zero air. The maximum of log-normal size distribution of aerosols is at a diameter of 100 nm.

To test the effect of this process, aerosols were added to the dilution flow of the calibration system. Zero air was humidified as described above to 78% relative humidity at room temperature in three experiments and dry zero air was used in the other experiment. Ammonium sulfate aerosols were produced by a collision-type atomizer<sup>14</sup> from a 1% solution in water. The size distribution was measured by a custom-designed differential mobility analyzer showing a center of the number distribution of  $\sim 100$  nm in all experiments. The aerosol concentration was determined by a standard particle counter. Both measurements together were used to estimate the mass load that was applied to the instrument.

Figure 6 shows the time evolution of the measured  $\text{N}_2\text{O}_5$  relative to the initial  $\text{N}_2\text{O}_5$ . A rapid decrease of the  $\text{N}_2\text{O}_5$  signal in all experiments can be observed, indicating that aerosol accumulation on the filter decreases the transmission efficiency. The measured  $\text{N}_2\text{O}_5$  signal returned to its initial value when the filter in the inlet system was changed indicating that accumulation of aerosols on the filter, rather than on the wall of the Teflon tubing, was responsible for the additional loss of  $\text{N}_2\text{O}_5$ . Thus, regular filter changes are necessary to prevent degradation of the transmission efficiency for  $\text{N}_2\text{O}_5$ .

All mass loads used during these experiments were large relative to typical ambient conditions.<sup>6,7,10</sup> The loss was  $\sim 3\%/min$  on dry aerosol at a mass load of  $30\,000\ \mu\text{g m}^{-3}$  and  $\sim 6\text{--}15$  times faster with a comparable mass load at relative humidity of 78% (Figure 6). At a typical mass load in polluted ambient air of  $\sim 20\ \mu\text{g m}^{-3}$ , a decrease of  $0.12\%/h$  is expected from a linear extrapolation for dry aerosol and a maximum of  $2.0\%/h$  for humid conditions. It can be concluded from these measurements that a filter change interval of 1 h is sufficient to avoid  $\text{N}_2\text{O}_5$  loss on the filter due to accumulation of aerosol under most conditions. However, the automatic filter changer system allows a change of filter more frequently if aerosol mass loadings are large. Alternatively, under conditions of low particle loading (e.g., remote locations or high altitude), the required interval for filter changes may be considerably longer than 1 h.

A similar test to that of  $\text{N}_2\text{O}_5$  uptake on aerosols was performed to investigate a possible decrease of the transmission efficiency of  $\text{NO}_3$  because of the interaction of  $\text{NO}_3$  with organic aerosols. The experiment was performed in the same way as that for the inorganic aerosol, but aerosols were produced from a adipic acid

**Table 1. Contribution to the  $1\sigma$  Accuracy of Measured Trace Gas Concentration**

	$\text{N}_2\text{O}_5$ (%)	$\text{NO}_3$ (%)	$\text{NO}_2$ (%)
cross section	$\pm 4$	$\pm 4$	$\pm 3$
$R_L$	$\pm 3$	$\pm 3$	$\pm 3$
inlet loss	$\pm 1$	$\pm 2$	na <sup>a</sup>
filter aging	+3	+3	na
sum	-8, +11	-9, +12	$\pm 6$

<sup>a</sup> na, not applicable.

solution in water (mass load,  $150\ \mu\text{g m}^{-3}$ ; maximum aerosol diameter, 100 nm). However, no decrease of the instrument's transmission efficiency could be observed over a sampling period of 1 h.

$\text{NO}_3$  is highly reactive toward many hydrocarbons.<sup>2</sup> We tested whether a degradation of the system's transmission efficiencies can be observed if a mixture of reactive hydrocarbons is sampled. A GC calibration standard (acetaldehyde 16.31 ppmv, ethanol 8.3 ppmv, *n*-pentane 7.89 ppmv, acetone 8.69 ppmv, and isoprene 7.21 ppmv) was diluted by a factor of 4000, resulting in a VOC mixing ratio of 12 ppbv. No significant changes of the measured transmission efficiencies for  $\text{NO}_3$  or  $\text{N}_2\text{O}_5$  could be observed when this mixture was sampled over a period of 6 h. Thus, reactive VOC does not appear to adsorb on the Teflon surfaces to a large enough extent to significantly affect the transmission efficiency.

## ACCURACY OF MEASUREMENTS

The accuracy of measurements achieved with this instrument is summarized in Table 1. In principle, the accuracy of  $\text{N}_2\text{O}_5$  and  $\text{NO}_2$  measurements also depend on the accuracy and the detection sensitivity with which  $\text{NO}_3$  and  $\text{O}_3$ , respectively, is measured, because only the sum of both is detected in this instrument. An explicit expression for taking this into account is given by refs 11 and 17 using error propagation. Here, accuracies are given for measurements of single species.

The overall  $1\sigma$  accuracy is determined by the uncertainties in the absorption cross section ( $\pm 4\%$ <sup>16,18,26</sup>), path length ratio ( $R_L$ ,  $\pm 3\%$ ), and transmission efficiencies (1% for  $\text{N}_2\text{O}_5$ , 2% for  $\text{NO}_3$ ). Because some of the errors in this sum are likely to be systematic (e.g., the absorption cross section and relative path length), we have added the contributions to the error linearly rather than in quadrature.

Although to our current understanding the decrease of transmission efficiencies due to the aging of the filter is small, if the filter in the inlet system is exchanged regularly, we add the standard deviation of the average of measured in-field calibrations during our last field mission (NO3Comp campaign in Juelich, Germany) as an upper limit of a possible filter aging. Filter aging adds a loss that would decrease the transmission efficiency. Therefore, this contribution to the accuracy is asymmetric and can only lead to an increased correction factor for  $\text{NO}_3$  and  $\text{N}_2\text{O}_5$  ( $+3\%$  for  $\text{NO}_3$  and  $\text{N}_2\text{O}_5$ ).

All contributions add up to an overall  $1\sigma$  accuracy for  $\text{N}_2\text{O}_5$  concentrations of  $-8, +11\%$ , for  $\text{NO}_3$  concentrations of  $-9, +12\%$  and for  $\text{NO}_2$  concentrations of  $\pm 8\%$ , where the  $\mp$  signs indicate that the actual value is low/high relative to the measurement.  $\text{NO}_3$  and  $\text{N}_2\text{O}_5$  measurements are now approximately twice as accurate compared to previous reported values ( $\pm 25\%$  for  $\text{NO}_3$  and  $\pm 20\%$

for  $\text{N}_2\text{O}_5^{11}$ ). The largest contribution to the error in the current instrument is now due to the uncertainty in the  $\text{NO}_3$  cross section itself rather than the inlet transmission efficiencies.

## SUMMARY

This article has described the further development of the NOAA pulsed cavity ring-down instrument used to measure simultaneously ambient  $\text{NO}_3$ ,  $\text{N}_2\text{O}_5$ , and  $\text{NO}_2$  concentrations with high sensitivity. The most important difference between previous descriptions of this instrument and that given in this paper include the following: (1) inclusion of four separate optical cavities, two each at 662 and 532 nm, with the 532-nm extinction measurements located immediately downstream in the sample flow from the 662-nm measurement; (2) reduction in the residence time of the sample air achieved by operating at reduced pressure and in narrower diameter tubing; and (3) inclusion of a calibration for inlet transmission efficiencies based on production of either  $\text{NO}_3$  or  $\text{N}_2\text{O}_5$  from a stable source followed by titration of  $\text{NO}_3$  to  $\text{NO}_2$ , which does not undergo significant loss in the instrument.

Possible losses of  $\text{NO}_3$  and  $\text{N}_2\text{O}_5$  were investigated via a series of laboratory tests. The overall  $\text{NO}_3$  transmission efficiency was found to be  $92 \pm 2\%$  while the  $\text{N}_2\text{O}_5$  conversion and transmission

efficiency is  $97 \pm 1\%$ . Both values are in agreement with an independent determination of the transmission efficiencies using our in-field calibration system (90, 97%, respectively). As a consequence, the accuracy has been significantly increased to  $-8$ ,  $+11\%$  for  $\text{N}_2\text{O}_5$  and  $-9$ ,  $+12\%$  for  $\text{NO}_3$ .

Several systematic tests were performed to investigate possible changes of the transmission efficiencies against specific contaminations found in ambient air. Whereas gas-phase contaminations do not affect instrument performance, accumulation of aerosols on the filter can lead to a significant decrease of the transmission efficiency of  $\text{N}_2\text{O}_5$ . This emphasizes that a regular change of the filter with an interval of  $\sim 1$  h is required to prevent that the transmission efficiency drops significantly with time for atmospherically relevant aerosol mass loads.

## ACKNOWLEDGMENT

This work was supported in part by NOAA's Atmospheric Chemistry and Climate Program.

Received for review April 11, 2008. Accepted May 16, 2008.

AC8007253